Journal of Geophysical Research: Biogeosciences

RESEARCH ARTICLE
10.1029/2018JG004439

Climate Variability Controls on CO_2 Consumption Fluxes and Carbon Dynamics for Monsoonal Rivers: Evidence From Xijiang River, Southwest China

Jun Zhong[1], Si-Liang Li[1], Jing Liu[2], Hu Ding[3], Xiaole Sun[4], Sheng Xu[5], Tiejun Wang[1], Rob M. Ellam[1,5], and Cong-Qiang Liu[1,3]

[1]Institute of Surface-Earth System Science, Tianjin University, Tianjin, China, [2]School of Management Science, Guizhou University of Finance and Economics, Guiyang, China, [3]State Key Laboratory of Environmental Geochemistry, Institute of Geochemistry, Chinese Academy of Sciences, Guiyang, China, [4]Baltic Sea Center, Stockholm University, Stockholm, Sweden, [5]Scottish Universities Environmental Research Centre, University of Glasgow, East Kilbride, UK

Key Points:
- Large temporal variabilities of major ions are observed through high-frequency sampling in the Xijiang River
- Multiple biogeochemical processes occur under various hydrological conditions, shifting $\delta^{13}C_{DIC}$ values in the catchment
- High discharge and temperature would increase mineral-water reaction rates and the CO_2 consumption fluxes

Supporting Information:
- Supporting Information S1

Correspondence to:
S.-L. Li,
siliang.li@tju.edu.cn

Citation:
Zhong, J., Li, S.-L., Liu, J., Ding, H., Sun, X., Xu, S., et al. (2018). Climate variability controls on CO_2 consumption fluxes and carbon dynamics for monsoonal rivers: Evidence from Xijiang River, Southwest China. *Journal of Geophysical Research: Biogeosciences*, *123*, 2553–2567. https://doi.org/10.1029/2018JG004439

Received 8 FEB 2018
Accepted 30 JUL 2018
Accepted article online 6 AUG 2018
Published online 27 AUG 2018

Abstract The feedbacks of climate variability on CO_2 consumption fluxes and carbon dynamics are thought to play an important role in moderating the global carbon cycle. High-frequency sampling campaigns and analyses were conducted in this study to investigate temporal variations of river water chemistry and the impacts of climate variability on CO_2 consumption fluxes and carbon dynamics for the Xijiang River, Southwest China. Physical processes modify biogeochemical processes, so major ions display different responses to changing discharge. The annual CO_2 consumption rate is $(6.8 \pm 0.2) \times 10^6$ ton/year by carbonate weathering and $(2.4 \pm 0.3) \times 10^6$ ton/year by silicate weathering. The annual CO_2 consumption flux is much higher than most world rivers, and strong CO_2 consumption capacities are observed in catchments in Southwest China. Lower negative $\delta^{13}C_{DIC}$ values are found in the high-flow season which corresponds with high temperatures compared to those in the low-flow season. High discharge will accelerate material transport, and high temperatures will increase primary production in the catchment, both of which can be responsible for the shift of $\delta^{13}C_{DIC}$ values in the high-flow season. Increased mineral weathering and biological carbon influx in the catchment are the main factors controlling carbon dynamics. Overall, these findings highlight the sensitivity of CO_2 consumption fluxes and carbon dynamics in response to climate variability in the riverine systems.

Plain Language Summary There are feedbacks between climate variability and CO_2 consumption fluxes by chemical weathering and carbon dynamics. Significant temporal variations of major ions and $\delta^{13}C_{DIC}$ are observed in the Xijiang River. Multiple biogeochemical processes occur under various hydrological conditions, shifting major ions concentrations, and $\delta^{13}C_{DIC}$. The annual CO_2 consumption rate is $(6.8 \pm 0.2) \times 10^6$ ton/year by carbonate weathering and $(2.4 \pm 0.3) \times 10^6$ ton/year by silicate weathering. The annual CO_2 consumption rates in the Xijiang River only account for a small fraction in the global CO_2 consumption rates; the CO_2 consumption capacity is much higher than the global average, while much lower than its source tributaries (Beipan and Nanpan Rivers). Slow subsurface flow paths with longer transit times switch to rapid near-surface flow paths with shorter transit times, as discharge increases. High temperatures increase reaction rates, and high discharge rates remove transport limitation, both of which would accelerate the chemical weathering rates. In the high-flow season, high discharge accompanying with high temperatures, large amounts of $\delta^{13}C$-depleted biological carbon, flushes into the river, affecting the carbon dynamics.

1. Introduction

Water chemistry in rivers offers valuable insights into chemical reactions, and physical and biogeochemical processes at catchment and regional scales, including mineral dissolution/precipitation, ion exchange, and nutrient transformation (Baronas et al., 2017; Hartmann et al., 2009; Kirchner & Neal, 2013; Maher & Chamberlain, 2014; Torres et al., 2016, 2015). Carbon and nutrient cycling on the Earth's surface is controlled by hydrological and biogeochemical processes (Burt et al., 2015; Gareis & Lesack, 2017; Raymond & Oh, 2007; Raymond et al., 2008; Reichstein et al., 2013), which can regulate the Earth's long-term climate though complex feedback mechanisms. Temperature and discharge are two critical expressive factors of climate variability, and changes in these factors can significantly alter flow regimes (Maher & Chamberlain, 2014; Raymond, 2017).

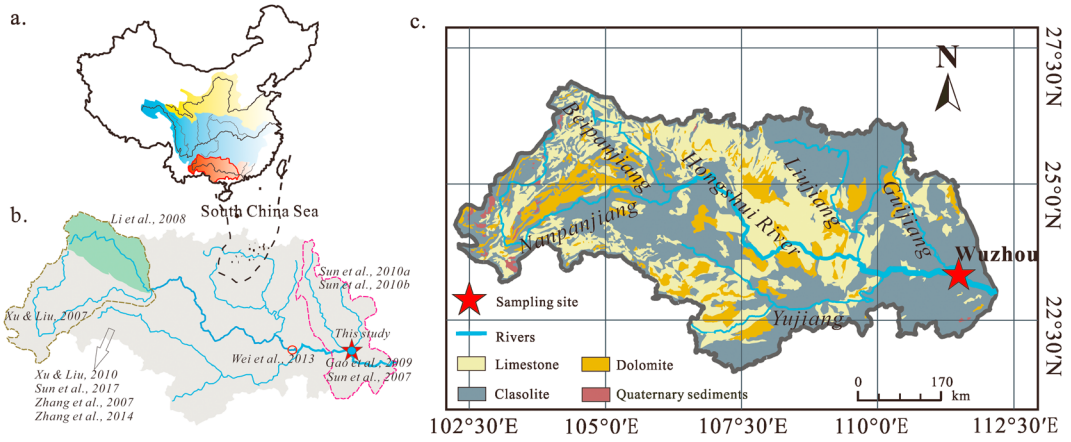

Figure 1. (a–c) Map showing the sampling locations of this study and previous studies in the Xijiang River and the geologic background of the study area.

Hydrological processes are major drivers that govern solute transport and carbon cycling through runoff generation processes that affect biogeochemical reactions (Cai et al., 2008; Kirchner & Neal, 2013; Maher & Chamberlain, 2014). For instance, previous studies have shown that concentration-discharge relationships can be useful in understanding solute transport (Basu et al., 2010; Burt et al., 2015; Godsey et al., 2009; Lloyd et al., 2016), source mixing (Calmels et al., 2011; Torres et al., 2016), and underlying biogeochemical reactions at catchment scales (Clow & Mast, 2010; Szramek et al., 2007; Torres et al., 2015; Zhong, Li, Tao, Ding, et al., 2017; Zhong, Li, Tao, Yue, et al., 2017). Temperature variability is another important factor affecting carbon cycles in river catchments. It is generally agreed that the rate of primary mineral dissolution is enhanced by increasing temperature (Goudie & Viles, 2012; Li et al., 2016), and associated microbial activities and chemical reactions are also highly affected by temperature variability (Liu & Xing, 2012). As such, temporal variations in solute chemistry in river water can reflect changes in related biogeochemical processes (Maher & Chamberlain, 2014; Musolff et al., 2017; Rue et al., 2017; Torres et al., 2015; Zhang et al., 2016). Numerous studies have highlighted the importance of temporal variations in major ions and chemical weathering at catchment scales, which are related to geological characteristics, geomorphology, hydrology, and human activities (Burt et al., 2015; Raymond et al., 2008; Tipper et al., 2006; Torres et al., 2015; Voss et al., 2014). As such, it is critical to obtain time series observations of relevant biogeochemical reactions to understand the complex interactions between the carbon cycle, chemical weathering processes, and hydrological processes (Kirchner & Neal, 2013; Tipper et al., 2006; Torres et al., 2015; Voss et al., 2014). In addition, accurate estimation of chemical weathering rates also depends on high temporal resolution of sampling and analysis (Moon et al., 2014; Zhong, Li, Tao, Ding, et al., 2017).

Major ion compositions and the carbon isotope compositions of dissolved inorganic carbon (DIC; $\delta^{13}C_{DIC}$) reflect dominant biological and chemical weathering processes (Barth et al., 2003; Hélie et al., 2002; Jin et al., 2014), which can be used to provide important information on carbon sources and chemical weathering in a catchment (Li et al., 2008, 2010; Marx et al., 2017; Telmer & Veizer, 1999; Zhong, Li, Tao, Yue, et al., 2017). Waldron et al. (2007) found that climate variability could alter the carbon mixed source compositions by controlling physical and biological processes in catchments. For example, changes in stream flow induced by climate variability affect physical processes in a catchment, which subsequently alter DIC compositions (Waldron et al., 2007). Carbon dynamics are highly affected by primary production, which is strongly moderated by temperature variability. Therefore, variations in climatic conditions may modify the relative carbon contributions from different potential sources (Liu & Xing, 2012; Marx et al., 2017), and therefore, carbon dynamics in rivers are sensitive to climate variability (Bouillon et al., 2014; Waldron et al., 2007). However, various biogeochemical processes underlying climate variability, especially behaviors of carbon, were insufficiently analyzed, and the effects of temperature and discharge on chemical weathering and carbon dynamics were poorly assessed.

The Xijiang River catchment in Southwest China is the world's largest Karst region with a typical monsoonal climate (Figure 1a). There have been several studies investigating chemical weathering processes in the

region based on spatial and temporal sampling campaigns (Li et al., 2008; Sun et al., 2017; Xu & Liu, 2007, 2010; Zhang et al., 2014), which analyzed water ion concentrations and carbon fluxes (Gao et al., 2009; Sun, Han, Li, et al., 2010; Sun, Han, Lu, et al., 2010), carbon dynamics in extreme precipitation events (Sun et al., 2007), and seasonal chemical weathering characteristics (Wei et al., 2013; Figure 1b). Significantly strong spatial and temporal variations of major ions were observed in these studies, and extreme precipitation had proved to exert strong effects on water chemistry. However, the impacts of climate variability on CO_2 consumption and carbon dynamics remain unclear in this region. In this study, we combine these previous studies with new results to (1) investigate the temporal variations in major ion concentrations and $\delta^{13}C_{DIC}$, (2) quantify the CO_2 consumption rates due to chemical weathering and analyze the effects of discharge change and temperature variability on CO_2 consumption fluxes, and (3) explore the control mechanisms of chemical weathering processes, biogeochemical processes, CO_2 consumption fluxes, and carbon dynamics under various climatic conditions for monsoonal rivers using samples collected at a high-frequency temporal resolution from the Xijiang River.

2. Materials and Methods

2.1. Study Area

The Yunnan-Guizhou Plateau is located in Southwest China in the center of the Southwest Asian Karst Region (Figure 1a), which is the largest karst area in the world. The Xijiang River has its source in the Maxiong Mountain to the west of Yunnan-Guizhou Plateau and flows southeast through the karst region, finally draining into the South China Sea. With a total length of 2,075 km and a drainage area of 353,120 km^2, the Xijiang River is the main tributary of the Zhujiang River (the second largest river in China in term of discharge), covering 77.8% of the whole drainage basin area and providing 63.9% of river discharge for the Zhujiang River.

The lithology of the upper Xijiang catchment is mainly carbonate ranging from Precambrian to Quaternary in age (Gao et al., 2009). Specifically, the strata exposed in the upper middle parts of the Xijiang catchment are mainly Permian and Triassic carbonate rocks (e.g., limestones and dolomites) and coal-bearing formations. The coal-bearing deposits are generally rich in sulfides (Li et al., 2008). Precambrian metamorphic rocks (e.g., schist and gneiss) and magmatic rocks (mainly granite) are dominant in the middle lower parts of the catchment. Jurassic detrital sedimentary rocks (mainly shales and red sandstones) are fragmentarily intercalated in the upper and middle areas (Liu, 2007). Abundant mineral deposits are found in the Xijiang catchment, with rich nonferrous metal resources. In the low reaches of the catchment, there are scattered occurrences of unconsolidated sediments. Red soil, limestone red soil, and lateritic red soil are mostly distributed in the Xijiang catchment (Xu & Liu, 2010). Minor evaporite deposits are scattered in the Xijiang catchment, and salt-bearing stratum has not been recorded in this area (Gao et al., 2009). Vegetation covers also varied considerably across the catchment with higher vegetation density in the middle areas (Xu & Liu, 2010).

Due to the Pacific Ocean and Indian Ocean monsoons, seasonal variations in air temperature and stream flow are highly correlated across the region (i.e., cold and dry weather in winter and warm and wet weather accompanied by frequent storms and typhoons in summer). Across the region, mean annual temperature ranges from 12 to 14 °C, and mean annual precipitation varies from 1,000 to 2,000 mm/year with an average of 80% of precipitation occurring from April to September (Liu, 2007). By the end of the year 2000, the average population density was about 170 persons per square kilometer in the whole catchment, with more than 300 persons per square kilometer in the source area (Xu & Liu, 2010). Anthropogenic activities are well developed in the upper reach of the catchment, with many dams constructed in the upper reach. In this study, the sampling site was chosen at the Wuzhou hydrologic station (Figure 1). About 91% of the catchment area and 94% of the total discharge of the Xijiang River drain through the Wuzhou station.

2.2. Sampling and Analytical Methods

Water samples were collected monthly at the Wuzhou hydrological station from October 2013 to September 2014 (Table S1 in the supporting information and Figure 1). Additional daily or weekly water samples were also collected during the high-flow season from June to September 2014, according to hydrological conditions. All samples were collected in the middle section of the river from a boat, thereby minimizing any influence from land-based pollution. Samples were first stored in high-density polyethylene container and then filtered through 0.45-μm Millipore nitrocellulose membrane filters within 24 hr of sampling. All containers

were prewashed with hydrochloric acid and rinsed with Milli-Q water in the laboratory before they were used in the field. In addition, in situ water temperature (*T*), pH, and electrical conductivity (EC) were measured when the samples were collected.

Alkalinity was determined by titration with 0.02-M hydrochloric acid within 24 hr of sampling. For cation analysis, a filtered solution was first acidified to pH = 2 using HNO_3 and then stored in pre-acid washed tubes. Major cations (i.e., K^+, Na^+, Ca^{2+}, and Mg^{2+}) were analyzed by inductively coupled plasma optical emission spectrometer, and major anions (i.e., Cl^-, SO_4^{2-}, and NO_3^-) were measured by ion chromatography. All the above analyses were conducted in the State Key Laboratory of Environmental Geochemistry, Institute of Geochemistry, Chinese Academy of Sciences, within a relative standard deviation (RSD) of 5%. For the analysis of $\delta^{13}C_{DIC}$, water samples were collected in polyethylene bottles with air-tight caps. A method modified from that described by Li et al. (2010) was adopted in this study: using 15-ml aliquots of the river water samples injected by syringes into glass bottles that were prefilled with 2-ml 85% phosphoric acid and magnetic stirrer bars. The CO_2 produced was then extracted in a vacuum line and transferred cryogenically into a glass tube for carbon isotopic measurements. The values of $\delta^{13}C_{DIC}$ were measured using a Finnigan MAT 252 mass spectrometer and were reported using the δ-notation relative to the Vienna Pee Dee Belemnite in permil, with an accuracy of 0.1‰. The pressure of dissolved CO_2 (pCO_2) in the water was calculated based on mass action relationships and the relative equilibrium constants (Clark & Fritz, 1997).

3. Results

3.1. Characteristics of Water Chemistry

The hydrology of the Xijiang River is affected by precipitation, ice and snow melting, and regulation of reservoirs. For the Wuzhou hydrological station, precipitation is the dominant control especially during the high-flow season (Fischer et al., 2013). In 2013, river discharge was low in October and separately peaked twice in the middle of November and December. Discharge then dropped quickly and stabilized at a minimum value until the high-flow season came with high but fluctuating discharge (Figure S1), corresponding to variable high precipitation in the high-flow season.

The river water is mildly alkaline during the whole hydrological year, with pH values from 7.3 to 7.9, so HCO_3^- is the main inorganic carbon species in riverine water (Clark & Fritz, 1997). As the dominant carbon species, DIC can be represented by HCO_3^- in the karst catchment (Cai et al., 2008; Hélie et al., 2002). The total dissolved solutes vary from 110 to 227 mg/L, with a discharge-weighted average ($\Sigma C \times Q/\Sigma Q$) of 160.1 mg/L, where *C* represents the concentration of various dissolved solutes and *Q* is the instantaneous discharge. It is about twice the global discharge-weighted average (i.e., 97 mg/L; Li & Bush, 2015) but much lower than that of the Wujiang River in the karst area in Southwest China (i.e., 265 mg/L; Zhong, Li, Tao, Yue, et al., 2017). The total cationic charge ($TZ^+ = Na^+ + K^+ + 2Ca^{2+} + 2Mg^{2+}$) varies from 1,401 to 3,138 μeq, which is about 1–3 times the average value of global large rivers (i.e., 1,250 μeq; Meybeck (1979)). The order of cation concentrations is $Ca^{2+} > Mg^{2+} > Na^+ > K^+$, with the sum of Ca^{2+} and Mg^{2+} accounting for more than 90% of TZ^+ in the Xijiang River. The total anionic charge ($TZ^- = HCO_3^- + Cl^- + 2SO_4^{2-} + NO_3^-$) varies from 1,428 to 2,828 μeq. The anion concentrations follow a decreasing order of $HCO_3^- > SO_4^{2-} > NO_3^- > Cl^-$, with the sum of HCO_3^- and SO_4^{2-} contributing over 87% of TZ^-. The normalized charge balance ($NICB = (TZ^+ - TZ^-)/(TZ^+ + TZ^-) \times 100\%$) provides quantitative information on the degree of inorganic charge imbalance, generally representing less than ±5% in this study. As shown in Figure S1, most of the major ions show significant temporal variations during the study period. In general, the concentrations of most major ions decreased considerably in the early stage of high-flow season (June and early July 2014) and then gradually recovered during the late stage of high-flow season (late July and August 2014). Ca^{2+} and HCO_3^- show relative more stable trends than other ions, and NO_3^-, which is highly affected by biological processes (e.g., nitrification and denitrification), shows no clear temporal variation pattern (Figures S1a, S1f, and S1i).

3.2. Temporal Variations in DIC and $\delta^{13}C_{DIC}$

During the entire hydrological year, DIC values ranged from 1,090 to 2,282 μmol/L, with higher concentrations in the low-flow season than in the high-flow season (Figure S1f). pCO_2 shows a strong dilution effect in the monsoon season, with a range from 1,169 to 5,391 μatm (Figure S1e), which is much higher than

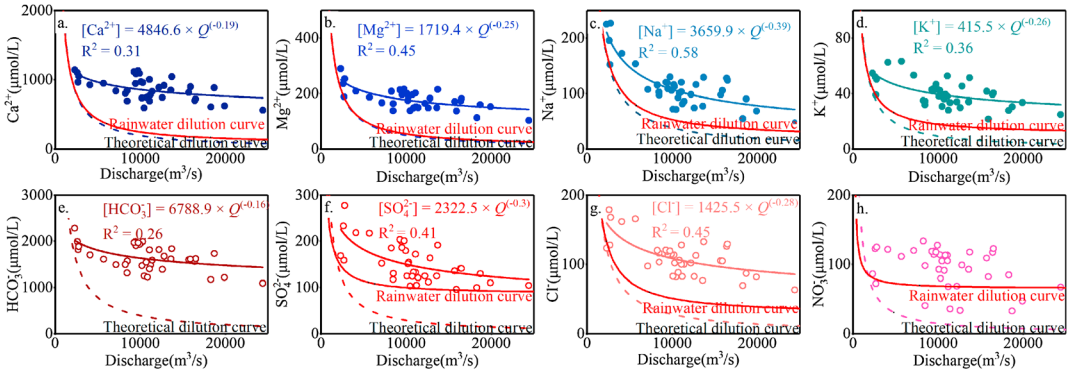

Figure 2. (a–h) Concentration-discharge relationships of major elements (Ca^{2+}, Mg^{2+}, Na^{+}, K^{+}, HCO_3^{-}, SO_4^{2-}, Cl^{-}, and NO_3^{-}). The theoretical dilution curve means that these elements are diluted by deionized water ($b = -1$), and the rainwater dilution curve means that these elements are diluted by rainwater in the catchment, which is accorded to Zhang et al. (2012).

that of the atmosphere (404 μatm; National Oceanic and Atmospheric Administration/Earth System Research Laboratory—Global Monitoring Division, 2016). $\delta^{13}C_{DIC}$ values show significant temporal trends, with $\delta^{13}C$-depleted values in the high-flow seasons (Figure S1j). $\delta^{13}C_{DIC}$ values change from −15.6‰ to −9.1‰ (Figure S1j), which is lower than −11.1‰ to −2.4‰ recorded in the Beipan River (Li et al., 2008) and the Guiping station, at the mainstream of the Xijiang River, with a range of −13‰ to −6.6‰ (Wei et al., 2013; Figure 1).

4. Discussions

4.1. Solute Concentration and Discharge Relationships (*C-Q*)

Previous studies have shown that concentrations of dissolved solutes in rivers in Southwest China, where monsoonal climates are prevalent, were highly related to changes in discharge (Li et al., 2010; Wei et al., 2013; Zhong, Li, Tao, Ding, et al., 2017). Similarly, water chemistry in the Xijiang River also reflects large seasonal variations in response to changes in river discharge (Figure 2). It is clear that concentrations of most ions are negatively correlated with river discharge. Higher concentrations are observed in the low-flow conditions due to the longer transit time of water within the catchment, while lower concentrations occur in the high-flow conditions with shorter transit time. The lower concentrations of these ions could be attributed to the dilution effect, which is consistent with the pattern of dissolved ion content variation with increasing discharge in humid subtropical rivers (Mortatti & Probst, 2003; Rai et al., 2010). Tipper et al. (2006) demonstrated that a modest dilution effect occurred when discharge exceeded base flow, because of the kinetic-limited weathering behavior of most dissolved solutes. In addition, the interaction of river water with the solid phase is another factor impacting water chemistry, and input of ion-rich soil water can trigger rock weathering processes (Clow & Mast, 2010; Covington et al., 2015; Hunsaker & Johnson, 2017; Maher & Chamberlain, 2014; Ran et al., 2013; Torres et al., 2015). Overall, the temporal patterns observed in the Xijiang River indicate that the major factors influencing the seasonal variations in major cations are the various chemical weathering rates and underlying biogeochemical processes under various climatic conditions. In addition, the seasonal variations in NO_3^{-} concentrations are greatly different from the seasonal patterns of other ions, with no significant dilution effect during the high-flow season (Figure S1), which is likely due to anthropogenic inputs and multiple biogeochemical processes as discussed below.

It should be noted that the response to river discharge change varies among the major ions as shown in Figure 2. The maximum Ca^{2+} and HCO_3^{-} concentrations are twice as high as their minimum concentrations. By comparison, the maximum Na^{+} and Cl^{-} concentrations are about 4 times higher than the minimum concentrations during the same study period. The concentrations of dissolved solutes are negatively correlated with river discharge, which can be expressed using a power function (Clow & Mast, 2010; Godsey et al., 2009):

$$C = a \times Q^{b} \quad (1)$$

where a is a constant and b indicates the deviation from dilution effect. Chemostatic behavior is introduced to represent phenomenon of the concentrations behaving stable relative to changes in discharge (Clow &

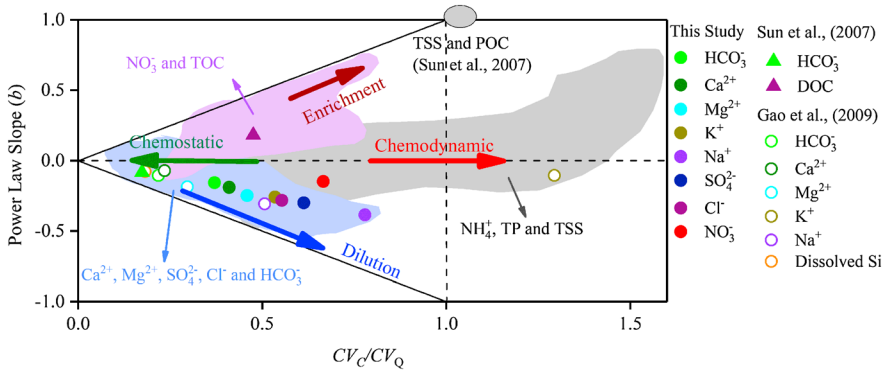

Figure 3. Plot of slope (b) versus CV_C/CV_Q for dissolved solutes of the Xijiang River and the shadow areas are from Bode River catchment (Musolff et al., 2015). TSS = total suspended sediment; POC = particulate organic carbon; DOC = dissolved organic carbon.

Mast, 2010). If $b = 0$, the solute behaves entirely chemostatically; whereas if $b = -1$, Q is the only control on C, and constant solute fluxes are diluted by variable fluxes of water (Zhong, Li, Tao, Ding, et al., 2017). If $-1 < b < 0$, both dilution and chemostatic behavior affect the solute concentrations. When $b > 0$, the dilution effect does not occur due to exogenous inputs brought by high discharge. Except for NO_3^-, power law negative relationships between major ion concentrations and river discharge are found for the Xijiang River (Figure 2).

As shown in Figure 2, the differences in the C-Q relationships indicate that different biogeochemical processes may have affected the behavior of various elements. The concentrations of Ca^{2+}, Mg^{2+}, and HCO_3^- do not temporally vary as much as Na^+, K^+, and Cl^- concentrations (Figure 2), indicating that Ca^{2+}, Mg^{2+}, and HCO_3^- exhibit stronger chemostatic responses, while Na^+, K^+, and Cl^- respond to the discharge change with a more significant dilution effect. The NO_3^- and SO_4^{2-} concentrations of some samples plot along or below the rainwater dilution curve, indicating that exogenous sources and biological processes might play an important part in shifting the concentrations of NO_3^- and SO_4^{2-}. The SO_4^{2-} concentrations in the Xijiang River are affected by anthropogenic inputs, precipitation, pyrite oxidation, and reduction of sulfate (Li et al., 2008), with pyrite oxidation being the main source of sulfate (Liu, 2007). The concentration of NO_3^- has no significant relation with river discharge (Figure 2e), which is likely because exogenous anthropogenic sources and relevant biogeochemical processes (e.g., nitrification and microbial activities) counteract the dilution effect.

Thompson et al. (2011) defined the following ratio between the coefficients of variation of concentration and discharge to provide an alternative parametric measure of chemostatic response:

$$CV_C/CV_Q = (\mu_Q/\mu_C) \times (\sigma_C/\sigma_Q) \quad (2)$$

where the coefficient of variation (CV) is the standard deviation (σ) of a variable normalized by its mean (μ). Incorporating equation (1), the CV ratio approximates the ratio of the standard deviations of C and Q. When no chemostatic response (dilution effect) exists, the value of b should be -1, resulting in $CV_C/CV_Q = 1$, which represents theoretical dilution by deionized water. Chemostatic behavior can then be considered as a special case, where the variability in concentration is highly buffered compared to the null hypothesis, that is, $CV_C/CV_Q << 1$ and b is close to 0. When concentration increases with discharge, flushing occurs, with $b > 0$. Meanwhile, in the case of $CV_C/CV_Q > 1$, the dissolved solutes show enrichment characteristics. Chemodynamic is a Q-independent status in which, despite a near-zero exponent b, the ratio of CV_C/CV_Q is high (Musolff et al., 2017, 2015) and indicates that although dissolved solute concentrations are highly dynamic, the C-Q relation is ambiguous.

Based on temporal variations in riverine ions, an export regime classification plot b versus CV_C/CV_Q was proposed to classify elements in rivers (Musolff et al., 2015). There are significant differences in the plot of b versus CV_C/CV_Q for various elements and catchments, which can reflect the sources and sinks of dissolved solutes and catchment-scale processes (Musolff et al., 2017, 2015). Ca^{2+}, Mg^{2+}, SO_4^{2-}, Cl^-, and HCO_3^- are located in the same range as those ions in the Bode River catchment, in central Germany, and K^+ is also located in the range as in the Bode River catchment (Figure 3). All of these ions are geologic solutes, which

are mainly derived from mineral weathering (Thompson et al., 2011). Carbonate weathering is the main source of HCO_3^-, Ca^{2+}, and Mg^{2+}, and the concentrations of these ions are highly controlled by the equilibrium of carbonate dissolution and precipitation, with $SI_{Calcite}$ index being unsaturated and saturated (Tipper et al., 2006; Zhong, Li, Tao, Ding, et al., 2017; Zhong, Li, Tao, Yue, et al., 2017). Therefore, these ions show near entirely chemostatic behavior, with near-zero *b* values and low CV_C/CV_Q ratios. Dissolved Si also shows strong chemostatic behavior (Figure 3), which can be ascribed to the equilibrium with respect to secondary silicate mineral and the retention and release of Si in the reservoir (Humborg et al., 1997; Maher & Chamberlain, 2014; Zhong, Li, Tao, Yue, et al., 2017). Na^+ mainly originates from silicate weathering (Gao et al., 2009) and shows more negative *b* values and higher CV_C/CV_Q ratios than other ions (Figure 3), which can be ascribed to the relatively stable main source of silicate weathering (Gao et al., 2009). K^+ also mainly comes from silicate weathering but is highly affected by cation exchange with the soil (Boy et al., 2008; Torres et al., 2015). Therefore, K^+ does not exhibit the same significant dilution effect observed for Na^+, especially showing chemodynamic behavior in extreme climate events (Gao et al., 2009). SO_4^{2-} and Cl^- show the dilution effect and chemodynamic behavior relative to Na^+, which can be attributed to the stable atmospheric and geologic sources, as well as anthropogenic inputs of these ions. The atmospheric and geologic sources would display a dilution effect, while the exogenous inputs counteract the dilution effect. The high CV_C/CV_Q ratio and near-zero *b* value for NO_3^- are caused by anthropogenic inputs, nitrification, and denitrification processes, which is different from the study in the Bode River catchment (Musolff et al., 2015). The total suspended sediment (TSS) and particulate organic carbon (POC) of extreme flood events in the Xijiang River display enrichment behavior (Figure 3), indicating that large amounts of soil (including organic carbon) are flushed into the river during flood events. All these observed plots of *b* versus CV_C/CV_Q ratio patterns can be explained by solute sources, the mineral dissolution kinetics, and the relative biogeochemical processes (Musolff et al., 2017).

4.2. The Impacts of Climate Variability on Chemical Weathering

Dissolved loads in rivers mainly originate from chemical weathering of various rocks and atmospheric and anthropogenic inputs (Gaillardet et al., 1999; Xu & Liu, 2007). The sum of Ca^{2+} and HCO_3^- accounts for approximately 70% of the total ions in the Xijiang River, suggesting that carbonate weathering is the dominant contributor of major ions in the river. These results are consistent with previous studies of the Xijiang River (Gao et al., 2009; Wei et al., 2013; Xu & Liu, 2007; Zhang et al., 2007), which also showed the predominance of carbonate weathering. Strong linear relationships of Mg^{2+}/Na^+ versus Ca^{2+}/Na^+ and SO_4^{2-}/Na^+ versus Ca^{2+}/Na^+ are found during the hydrological year (Figure 4). Carbonate weathering is the main source of Ca^{2+} and Mg^{2+}, and silicate weathering is the main source of Na^+ (Gao et al., 2009). Although rainwater has lower Ca^{2+}/Na^+ (averaged at 3.6) and Mg^{2+}/Na^+ (averaged at 0.4) ratios (Table S2), higher ratios of Ca^{2+}/Na^+ and Mg^{2+}/Na^+ under high-flow conditions indicate higher contribution ratios from carbonate weathering in high-flow conditions compared to in low-flow conditions. Because of differences in dissolution and precipitation kinetics, various behaviors of carbonate and silicate mineral weathering to changing discharge may occur (Tipper et al., 2006; Zhong, Li, Tao, Ding, et al., 2017; Zhong, Li, Tao, Yue, et al., 2017). Ca^{2+} concentrations decrease more slowly than Na^+ concentrations in response to increasing river discharge, which suggests stronger chemostatic behavior of carbonate weathering (indicated by Ca^{2+}) than silicate weathering (indicated by Na^+). Carbonate weathering is dominant in the Xijiang River, especially in the Beipan River (Figure 4a). For SO_4^{2-} atmospheric input cannot be neglected, with rainwater having higher SO_4^{2-}/Na^+ ratios (averaged at 4.9) relative to the river water (Table S2). SO_4^{2-}/Na^+ and Ca^{2+}/Na^+ ratios in the river water are much lower than the lines of carbonate weathering by H_2SO_4 and gypsum dissolution (Figure 4b), especially, under high-flow conditions. H_2SO_4 is a critical agent in carbonate weathering in Southwest China (Li et al., 2008; Xu & Liu, 2007) which can be mainly produced naturally through the oxidation of pyrite (Li et al., 2008; Liu, 2007; Xu & Liu, 2010). SO_4^{2-}/Na^+ and Ca^{2+}/Na^+ ratios are similar to other studies in the Xijiang catchment (Gao et al., 2009; Sun, Han, Li, et al., 2010; Sun et al., 2017; Wang et al., 2015; Wei et al., 2013; Xu & Liu, 2007, 2010) and overlap the range throughout the world (Figure 4b). However, the Xijiang River is more highly affected by carbonate weathering and by the action of H_2SO_4 than most rivers in the world (Figure 4b).

Based on forward methods described in the supporting information (Rai et al., 2010), the sources of major ions can be identified, and the CO_2 consumption fluxes (FCO_2) can be estimated (supporting information).

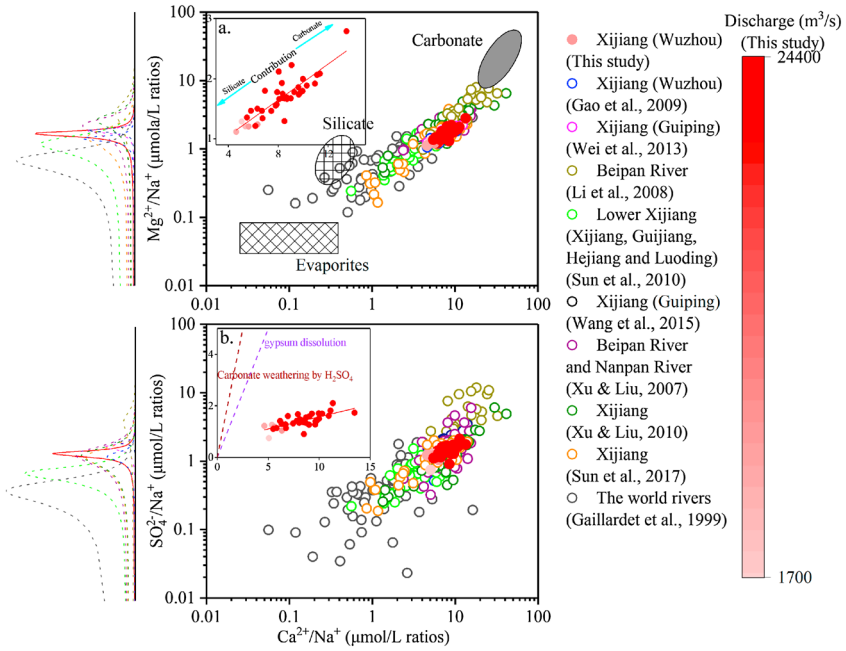

Figure 4. (a) The relationships of Mg^{2+}/Na^{+} versus Ca^{2+}/Na^{+}. (b) The correlation of SO_4^{2-}/Na^{+} versus Ca^{2+}/Na^{+}.

We use an improved index relative to the measured discharge and temperature to quantify the temporal discharge dynamics and water temperature dynamics. The discharge and water temperature are normalized using the following equations:

$$\text{Normalized discharge} = (Q_i - Q_{\min})/(Q_{\max} - Q_{\min}) \tag{3}$$

$$\text{Normalized temperature } (NT) = (T_i - T_{\min})/(T_{\max} - T_{\min}) \tag{4}$$

where Q_i and T_i are the respective discharge rate and instantaneous water temperature at time i, $Q_{\max}$ and $T_{\max}$ are the respective maximum discharge rate and water temperature of all available records, and $Q_{\min}$ and $T_{\min}$ are the respective minimum discharge rate and water temperature of all available records.

TZ^{+}_{Carb} represents TZ^{+} from carbonate weathering (equation (S2)), and TZ^{+}_{Sil} represents TZ^{+} from silicate weathering (equation (S3)). A positive correlation between $TZ^{+}_{Carb}/TZ^{+}_{Sil}$ ratios and normalized discharge is observed (Figure 5a), and TZ^{+}_{Sil} has a stronger dilution effect and higher sensitivity to changes in river discharge than TZ^{+}_{Carb} (Figure S2). Concentrations of carbonate weathering products show relatively little variations with discharge change, possibly due to higher mineral dissolution rates (Calmels et al., 2011; Tipper et al., 2006;

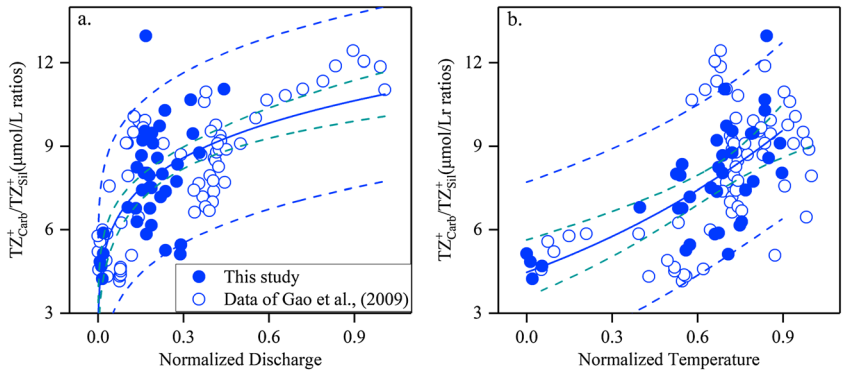

Figure 5. (a) Relationships between $TZ^{+}_{Carb}/TZ^{+}_{Sil}$ ratios and normalized discharge. (b) Relationship between $TZ^{+}_{Carb}/TZ^{+}_{Sil}$ ratios and normalized discharge for the Xijiang River.

Table 1
CO_2 Consumption for the Xijiang River in This Study and Other Studies

Rivers	Area 10^4 km^2	Discharge km^3/year	$[RCO_2]_{Carb}$ 10^6ton/year	$[RCO_2]_{Sil}$ 10^6ton/year	References
Xijiang	32.7	215	6.8 ± 0.2	2.4 ± 0.3	This study
Xijiang	35.2	230	12.5	2.4	Xu and Liu (2010)
Xijiang	43.7	363	12.5	1.1	Gaillardet et al. (1999)
Xijiang	35.3	230	18.5	5.3	Gao et al. (2009)
Xijiang	35.2	218.1	13.0	6.1	Sun, Han, Li, et al. (2010)

Zhong, Li, Tao, Yue, et al., 2017). Similar behavior was observed in climatically diverse global rivers (Calmels et al., 2011; Moon et al., 2014; Tipper et al., 2006). This suggests that dissolved solutes in rivers with high discharge and short residence time may have higher contributions from carbonate weathering (Moon et al., 2014). It has long been recognized that temperature is an important parameter, affecting chemical weathering (Gaillardet et al., 1999; Goudie & Viles, 2012; Li et al., 2016; Raymond, 2017). However, it is not easy to demonstrate the dependence of chemical weathering on temperature, because of its codependence with other factors that also affect weathering, such as evaporation, precipitation, and land cover (Goudie & Viles, 2012). TZ^+_{Carb}/TZ^+_{Sil} ratios have a positive relationship with normalized temperature (Figure 5b). TZ^+_{Carb} is more sensitive to temperature variability than TZ^+_{Sil}, which could be attributed to the faster dissolution kinetics of carbonate allowing a higher proportion of carbonate dissolution with increasing temperature (Tipper et al., 2006).

4.3. CO_2 Consumption Fluxes

The covariation between dissolved solute concentration and discharge induces large uncertainties in estimating annual CO_2 consumption rates (RCO_2) (Moon et al., 2014). Time series sampling and analyses were used in this study to reduce the estimation uncertainty. RCO_2 was calculated using the USGS LoadEst program (Runkel et al., 2004), with data files processed by the LoadRunner program (Booth et al., 2007). Based on Akaike Information Criterion (Booth et al., 2007), we selected the following model to estimate the CO_2 consumption rates in Xijiang River.

$$\ln Load = a_0 + a_1 \ln Q + a_2 \sin(2\,\pi\, dtime) + a_3 \cos(2\,\pi\, dtime) \quad (5)$$

where *Load* = constituent fluxes (kg/d), ln*Q* = ln (*Q*) − center of ln (*Q*), and *dtime* = decimal time − center of decimal time. The LoadEst program performs calibration procedures and estimates fluxes using the adjusted maximum likelihood estimation algorithm.

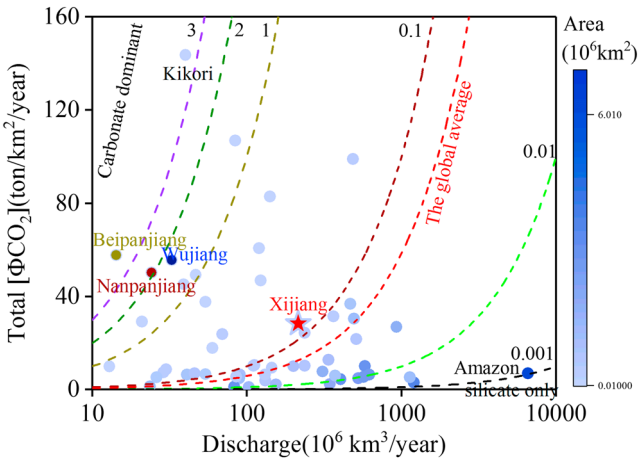

Figure 6. The relationship between total [ΦCO$_2$] and discharge for global rivers. The global [ΦCO$_2$] data were from Gaillardet et al. (1999); the data of Nanpanjiang, Beipanjiang, and Wujiang were from Xu and Liu (2007). The dashed lines represent the CO_2 consumption capacity, which is defined as total [ΦCO$_2$]/Discharge.

The calculated $[RCO_2]_{Carb}$ (The annual CO_2 consumption rate by carbonate weathering) is (6.8 ± 0.2) × 10^6 ton/year, and the $[RCO_2]_{Sil}$ (The annual CO_2 consumption rate by silicate weathering) is (2.4 ± 0.3) × 10^6 ton/year, accounting for about 1.26% of the global $[RCO_2]_{Carb}$ and 0.47% of the global $[RCO_2]_{Sil}$ (Gaillardet et al., 1999). The calculated $[RCO_2]_{Carb}$ of the Xijiang River in our study is similar to the values reported by Gaillardet et al. (1999) and Xu and Liu (2010) but much lower than that from Gao et al. (2009) and Sun, Han, Li, et al. (2010). The calculated $[RCO_2]_{Sil}$ is also similar to Xu and Liu (2010) but much lower than that from Gao et al. (2009) and Sun, Han, Li, et al. (2010) and higher than that from Gaillardet et al. (1999; Table 1). The $[RCO_2]_{Carb}$ and $[RCO_2]_{Sil}$ values reported from previous studies were estimated either from rather limited sampling campaigns or from sampling in extreme hydrological years, both of which lead to substantial uncertainties in the estimation.

River flow is needed to transport the weathered solutes, and discharge thus has a crucial role in chemical weathering fluxes, as well as total CO_2 consumption fluxes [ΦCO$_2$] ($[\Phi CO_2]_{Carb}$ + $[\Phi CO_2]_{Sil}$), which is defined as [RCO_2] of unit area. The total [ΦCO$_2$] in the Xijiang River is higher than most rivers in the world (Figure 6) but actually much lower than other rivers in Southwest China (Figure 6). On a global basis, rivers with large

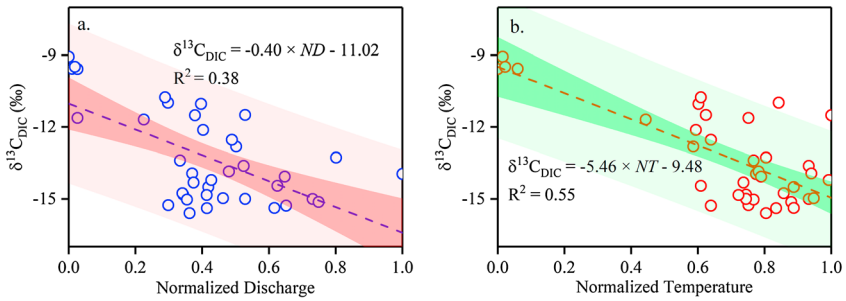

Figure 7. (a) Plots showing the relationship between $\delta^{13}C_{DIC}$ and normalized discharge. (b) The relationship between $\delta^{13}C_{DIC}$ and normalized temperature for the water collected from Xijiang River.

drainage areas extent usually have lower total [ΦCO_2] and higher CO_2 consumption capacity generally than rivers with low discharge and small drainage areas. The Xijiang River exhibited a higher CO_2 consumption capacity than the global average; however, the Beipan, Nanpan, and Wujiang Rivers, which are also located in the karst area of Southwest China, showed much higher CO_2 consumption capacities (Figure 6). As the upper stream tributaries of the Xijiang River, the Beipan and Nanpan Rivers showed high CO_2 consumption capacities (Figure 6). For comparison, the Amazon River which has the world's highest discharge and largest area also shows the lowest CO_2 consumption capacity (Figure 6). In general, rivers with higher discharge and larger areas usually have lower CO_2 consumption capacity. When the transit time in the weathering environment is much longer than the reaction time, mineral weathering is controlled by transport limitation (West et al., 2005). In contrast, reaction limitation is the main controller on chemical weathering (West et al., 2005). Chemical weathering capacity is a direct index to represent the controls on chemical weathering. High chemical weathering capacity corresponds to intense transport limitation. Large rivers with high discharge and low [ΦCO_2] are highly affected by reaction limitation, such as Amazon. Karst rivers in Southwest China are affected by transport limitation.

4.4. Carbon Dynamics and the Controlling Factors

Total carbon (TC), DIC, POC, and dissolved organic carbon (DOC) fluxes show increasing trends with increasing discharge (Figure S4). While fluxes of TC, DIC, and DOC show positive linear relationships with discharge (Figures S4a, S4b, and S4d), the POC flux follows a positive power law relationship with increasing discharge with $b > 1$ (Figure S4c), accounting for the high POC content induced by high discharge (Sun, Han, Lu, et al., 2010). TC flux is dominated by DIC flux (ranging from 80.7% to 89.3%) in the Xijiang River. Therefore, the DIC dynamics in the Xijiang River are critical to investigating the carbon cycle in the Xijiang catchment.

Although DIC concentrations show strong chemostatic behavior in response to discharge change (Figure 3), temporal DIC dynamics and compositions are affected by variability in discharge (Liu & Xing, 2012; Waldron et al., 2007; Zhong, Li, Tao, Yue, et al., 2017). $\delta^{13}C_{DIC}$ is a particularly useful tool for investigating the underlying fluvial carbon biogeochemical processes under various discharge changes, and the $\delta^{13}C_{DIC}$ values can be related to changes in carbon sources (Liu & Xing, 2012; Waldron et al., 2007), which can increase the uncertainties of source discrimination (Marx et al., 2017). Waldron et al. (2007) found that $\delta^{13}C_{DIC}$ respond more sensitively than DIC concentration to discharge change. The fluvial DIC dynamics reflect the changing mixture of compositionally distinct pools whose contributions have altered DIC composition (Li et al., 2010; Liu & Xing, 2012; Waldron et al., 2007; Zhong, Li, Tao, Yue, et al., 2017). The mixing of end-members is not compositionally constant, and both biological and physical processes alter the mixed source composition (Waldron et al., 2007). Therefore, high-temporal resolution $\delta^{13}C_{DIC}$ data were analyzed to approximate source mixing and relevant biogeochemical processes. Figure S1 shows that lower $\delta^{13}C_{DIC}$ values occur in the high-flow season, while higher $\delta^{13}C_{DIC}$ values occur in the low-flow season, as more soil-derived water contributes to the discharge in response to heavy precipitation in the high-flow season (Waldron et al., 2007). These observations agree with previous studies (Hélie et al., 2002; Li et al., 2010; Liu & Xing, 2012; Waldron et al., 2007; Wei et al., 2013; Zhong, Li, Tao, Yue, et al., 2017).

A negative linear relationship between $\delta^{13}C_{DIC}$ and normalized discharge is observed (Figure 7a), showing that lower $\delta^{13}C_{DIC}$ values are associated with high discharge conditions. Slow subsurface flow paths with

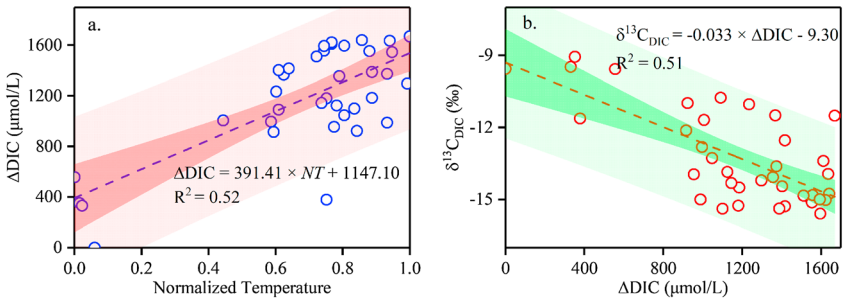

Figure 8. (a) Plot between ΔDIC and normalized temperature. (b) Plot between $\delta^{13}C_{DIC}$ and ΔDIC. DIC = dissolved inorganic carbon.

longer transit times would switch to rapid near-surface flow paths with shorter transit times, as discharge increases (Calmels et al., 2011; Tipper et al., 2006; Torres et al., 2015). Large amounts of δ^{13}C-depleted carbon are stored in the epikarst waters (Li et al., 2010), which are released by high discharge. Meanwhile, high soil CO_2 content would be released by high discharge and then flush into the river. The higher contribution of δ^{13}C-depleted soil CO_2 into the river induced by high discharge would shift $\delta^{13}C_{DIC}$ to more negative values. There is a significant negative relationship between $\delta^{13}C_{DIC}$ and normalized temperature for the water collected in the Xijiang River (Figure 7b). With increasing temperature, plant cover is relatively high, plant production increases in the catchment, bacterial activity is strong, and the decomposition of soil organic materials also increases (Liu & Xing, 2012). In contrast, at low temperatures the plant cover is reduced, and bacteria activity is weakened (Liu & Xing, 2012). Therefore, the productivity of soil CO_2 increases with high temperatures, accounting for the high soil CO_2 contribution to the riverine water.

ΔDIC is defined as the difference between measured DIC value and the theoretical DIC value (from the theoretical dilution curve), predicted for exogenous sources:

$$\Delta DIC = DIC_{measured} - DIC_{theoretical} \quad (6)$$

DIC shows strong chemostatic behavior in response to discharge change, indicating that high contents of exogenous DIC are flushed into the river when discharge increases. A positive relationship exists between ΔDIC and normalized temperature, showing that temperature plays an important role in controlling exogenous DIC inputs. A negative relationship between $\delta^{13}C_{DIC}$ and ΔDIC is observed for the water collected in the Xijiang River (Figure 8b), indicating that the input of δ^{13}C-depleted exogenous DIC plays an important role in shaping DIC concentrations. The intense precipitation in Southwest China is always accompanied by high temperatures, prompting to the high-flow season. Therefore, high river discharge in the summer could flush away lower $\delta^{13}C_{DIC}$ water stored in soil matrix porosity to the river (Li et al., 2010). The monitoring of soil CO_2 in Southwest China has shown that soil CO_2 was higher than 3×10^5 ppm in summer and higher than 4×10^3 ppm in winter (Liu, 2007). The dissolution of soil CO_2 with negative δ^{13}C values during the high-flow season is the major factor affecting $\delta^{13}C_{DIC}$ values in the Xijiang River. In addition, abundant terrestrial organic matter is also transported into the river by physical processes during high river discharge (Gao et al., 2009). On the other hand, large amounts of organic materials are mineralized to DIC after several days of incubation at ambient river temperature (Ward et al., 2013). Therefore, the degradation of organic matter in rivers could be another factor that influences the $\delta^{13}C_{DIC}$ values. CO_2 degassing occurs along the rivers (Raymond et al., 2013), which would shift lower DIC concentrations and δ^{13}C-riched values. The water travel time in river channel is long in low-flow season, which would lead to higher $\delta^{13}C_{DIC}$ and lower DIC concentrations. However, the effect of CO_2 degassing on carbon temporal variations is not as significant as the effects of mineral weathering and biological CO_2 influx. Overall, mineral weathering, soil CO_2 influx, and degradation of organic matter in the river are responsible for the carbon temporal dynamics in the Xijiang River.

4.5. Sensitivity of [FCO_2] and DIC Flux (F_{DIC}) to Discharge and Temperature Changes for the Xijiang River

It has long been accepted that climate variability is expected to play a crucial role in the global carbon cycling (Calmels et al., 2011; Clow & Mast, 2010; Goudie & Viles, 2012; Liu & Xing, 2012; Tipper et al., 2006; Zhong, Li, Tao, Yue, et al., 2017). The feedback of climate variability on carbon cycling is complex and needs to be further

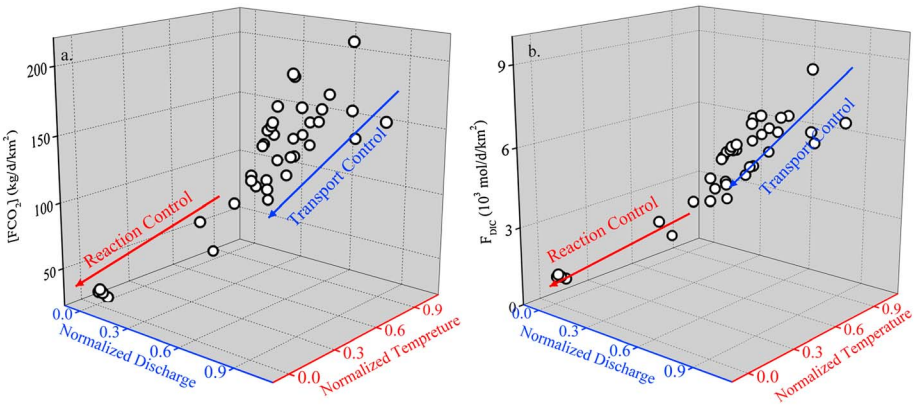

Figure 9. (a) Three-dimensional representation of the [FCO_2] along the normalized discharge and normalized temperature. (b) Three-dimensional representation of F_{DIC} along the normalized discharge and normalized temperature for the water collected in the Xijiang River.

investigated. As discussed above, both high discharge and high temperatures lead to an acceleration of chemical weathering and DIC fluxes (F_{DIC} = DIC concentration × discharge). High temperatures will enhance the primary mineral dissolution by increasing chemical weathering reactions. High discharge will transport the chemical weathering materials and enhance the available mineral-water reaction surface; the transit time is much shorter than the reaction time (West et al., 2005). For the low-flow season, the discharge change is low and the temperature variability is high (except during extreme climate events, such as occasional high precipitation); [FCO_2] (Eq. S4 & S5) and F_{DIC} are more sensitive to temperature variability than discharge change (Figure 9). However, the discharge change is high, and the temperature varies in a narrow range, so the effects of discharge change could conceal any temperature dependence, so that discharge change has a much higher impact on [FCO_2] and F_{DIC} in the high-flow conditions (Figure 9). On the whole, although both discharge and temperature shape [FCO_2] and F_{DIC}, because of the high discharge change and low temperature variability, discharge change always plays a more significant role on [FCO_2] and F_{DIC} than temperature variability.

5. Conclusions

This study provides insights on the effects of climate variability on CO_2 consumption fluxes and carbon dynamics in monsoonal rivers, based on high-frequency variations in dissolved solutes and $\delta^{13}C_{DIC}$ values of riverine water in a hydrological year.

The dissolved solutes show significant temporal variations during the entire hydrological year. The concentrations of most elements decrease with increasing river discharge due to the dilution effect. However, they do not behave similar and do not follow the dilution curve closely, because of ions exchange, mineral dissolution/precipitation, and biological processes. Carbonate is widely distributed in the catchment, and carbonate weathering acts as the major source for dissolved solutes. Ions from carbonate weathering showed stronger chemostatic behavior to discharge change than silicate weathering, which can be attributed to the rapid dissolution and precipitation characteristics of carbonate minerals. Due to the strong biological reaction in the catchment, NO_3^- showed significant chemodynamic behavior. CO_2 consumption fluxes increase with increasing river discharge, due to the increased available reaction surface. Based on the LoadEst program, the annual CO_2 consumption rates are calculated to be $(6.8 \pm 0.2) \times 10^6$ ton/year and $(2.4 \pm 0.3) \times 10^6$ ton/year for carbonate weathering and silicate weathering, respectively. The annual CO_2 consumption rates in the Xijiang River only accounted for a small fraction in the global CO_2 consumption rates, while the CO_2 consumption capacity was much higher than the global average.

Primary production in the catchment is increased when the temperature is high, and large amounts of organic materials are produced. Meanwhile, the degradation of organic materials is increased at moderate temperature. Slow subsurface flow paths with longer transit times switch to rapid near-surface flow paths with shorter transit times, as discharge increases. Although high discharge dilutes the carbon

concentration, large amounts of $\delta^{13}C$-depleted soil carbon are flushed into the river in the high-flow season. The transport of mineral weathering materials, influx of $\delta^{13}C$-depleted soil CO_2, and degradation of organic matter in rivers are the main factors controlling the carbon dynamics. The CO_2 consumption fluxes and F_{DIC} are affected by both discharge change and temperature variability. The discharge change is low, and the temperature variability is high in the low-flow season. Therefore, the CO_2 consumption fluxes and F_{DIC} are highly affected by reaction control in the low-flow season. The discharge change is large, and the water temperature was constant in the high-flow season. So transport control is the main driver of CO_2 consumption fluxes and F_{DIC}. We suggest that the sensitivity of CO_2 consumption fluxes and carbon dynamics to climate variability is significant in monsoonal rivers. More attentions should be concentrated on distinguishing the contributions of discharge change and temperature variability on CO_2 consumption fluxes and carbon dynamics in future studies.

Acknowledgments
This work is financially supported by the National Key R & D Program of China through grant 2016YFA0601002 and the National Natural Science Foundation of China (grants 41422303, 41571130072, and 41130536). Data are provided in the figures and the table in the text and the supporting information. Discharge data were obtained online from the Ministry of Water Resources (http://www.hydro-info.gov.cn/).

References

Baronas, J. J., Torres, M. A., Clark, K. E., & West, A. J. (2017). Mixing as a driver of temporal variations in river hydrochemistry: 2. Major and trace element concentration dynamics in the Andes-Amazon transition. *Water Resources Research*, *53*, 3120–3145. https://doi.org/10.1002/2016WR019729

Barth, J. A. C., Cronin, A. A., Dunlop, J., & Kalin, R. M. (2003). Influence of carbonates on the riverine carbon cycle in an anthropogenically dominated catchment basin: Evidence from major elements and stable carbon isotopes in the Lagan River (N. Ireland). *Chemical Geology*, *200*(3–4), 203–216. https://doi.org/10.1016/S0009-2541(03)00193-1

Basu, N. B., Destouni, G., Jawitz, J. W., Thompson, S. E., Loukinova, N. V., Darracq, A., et al. (2010). Nutrient loads exported from managed catchments reveal emergent biogeochemical stationarity. *Geophysical Research Letters*, *37*, L23404. https://doi.org/10.1029/2010GL045168

Booth, G., Raymond, P., & Oh, N.-H. (2007). LoadRunner. New Haven, CT. Retrieved from http://environment.yale.edu/raymond/loadrunner

Bouillon, S., Yambélé, A., Gillikin, D. P., Teodoru, C., Darchambeau, F., Lambert, T., & Borges, A. V. (2014). Contrasting biogeochemical characteristics of the Oubangui River and tributaries (Congo River basin). *Scientific Reports*, *4*(1), 5402. https://doi.org/10.1038/srep05402

Boy, J., Valarezo, C., & Wilcke, W. (2008). Water flow paths in soil control element exports in an Andean tropical montane forest. *European Journal of Soil Science*, *59*(6), 1209–1227. https://doi.org/10.1111/j.1365-2389.2008.01063.x

Burt, T. P., Worrall, F., Howden, N. J. K., & Anderson, M. G. (2015). Shifts in discharge-concentration relationships as a small catchment recover from severe drought. *Hydrological Processes*, *29*(4), 498–507. https://doi.org/10.1002/hyp.10169

Cai, W. J., Guo, X. H., Chen, C. T. A., Dai, M. H., Zhang, L. J., Zhai, W. D., et al. (2008). A comparative overview of weathering intensity and HCO_3^- flux in the world's major rivers with emphasis on the Changjiang, Huanghe, Zhujiang (Pearl) and Mississippi Rivers. *Continental Shelf Research*, *28*(12), 1538–1549. https://doi.org/10.1016/j.csr.2007.10.014

Calmels, D., Galy, A., Hovius, N., Bickle, M., West, A. J., Chen, M. C., & Chapman, H. (2011). Contribution of deep groundwater to the weathering budget in a rapidly eroding mountain belt, Taiwan. *Earth and Planetary Science Letters*, *303*(1–2), 48–58. https://doi.org/10.1016/j.epsl.2010.12.032

Clark, I., & Fritz, P. (1997). *Environmental isotopes in hydrogeology*. Boca Raton, FL: Lewis Publishers.

Clow, D. W., & Mast, M. A. (2010). Mechanisms for chemostatic behavior in catchments: Implications for CO_2 consumption by mineral weathering. *Chemical Geology*, *269*(1–2), 40–51. https://doi.org/10.1016/j.chemgeo.2009.09.014

Covington, M. D., Gulley, J. D., & Gabrovšek, F. (2015). Natural variations in calcite dissolution rates in streams: Controls, implications, and open questions. *Geophysical Research Letters*, *42*, 2836–2843. https://doi.org/10.1002/2015gl063044

Fischer, T., Gemmer, M., Su, B., & Scholten, T. (2013). Hydrological long-term dry and wet periods in the Xijiang River basin, South China. *Hydrology and Earth System Sciences*, *17*(1), 135–148, https://doi.org/10.5194/hess-17-135-2013

Gaillardet, J., Dupré, B., Louvat, P., & Allegre, C. J. (1999). Global silicate weathering and CO_2 consumption rates deduced from the chemistry of large rivers. *Chemical Geology*, *159*(1–4), 3–30. https://doi.org/10.1016/S0009-2541(99)00031-5

Gao, Q., Tao, Z., Huang, X., Nan, L., Yu, K., & Wang, Z. (2009). Chemical weathering and CO_2 consumption in the Xijiang River basin, South China. *Geomorphology*, *106*(3–4), 324–332. https://doi.org/10.1016/j.geomorph.2008.11.010

Gareis, J. A., & Lesack, L. F. (2017). Fluxes of particulates and nutrients during hydrologically defined seasonal periods in an ice-affected great Arctic river, the Mackenzie. *Water Resources Research*, *53*, 6109–6132. https://doi.org/10.1002/2017WR020623

Godsey, S. E., Kirchner, J. W., & Clow, D. W. (2009). Concentration-discharge relationships reflect chemostatic characteristics of US catchments. *Hydrological Processes*, *23*(13), 1844–1864. https://doi.org/10.1002/hyp.7315

Goudie, A. S., & Viles, H. A. (2012). Weathering and the global carbon cycle: Geomorphological perspectives. *Earth-Science Reviews*, *113*(1–2), 59–71. https://doi.org/10.1016/j.earscirev.2012.03.005

Hartmann, J., Jansen, N., Dürr, H. H., Kempe, S., & Köhler, P. (2009). Global CO_2-consumption by chemical weathering: What is the contribution of highly active weathering regions? *Global and Planetary Change*, *69*(4), 185–194. https://doi.org/10.1016/j.gloplacha.2009.07.007

Hélie, J.-F., Hillaire-Marcel, C., & Rondeau, B. (2002). Seasonal changes in the sources and fluxes of dissolved inorganic carbon through the St. Lawrence River—isotopic and chemical constraint. *Chemical Geology*, *186*, 117–138. https://doi.org/10.1016/S0009-2541(01)00417-X

Humborg, C., Ittekkot, V., Cociasu, A., & Bodungen, B. V. (1997). Effect of Danube River dam on Black Sea biogeochemistry and ecosystem structure. *Nature*, *386*(6623), 385–388. https://doi.org/10.1038/386385a0

Hunsaker, C. T., & Johnson, D. W. (2017). Concentration-discharge relationships in headwater streams of the Sierra Nevada, California. *Water Resources Research*, *53*, 7869–7884. https://doi.org/10.1002/2016wr019693

Jin, J., Zimmerman, A. R., Moore, P. J., & Martin, J. B. (2014). Organic and inorganic carbon dynamics in a karst aquifer: Santa Fe River Sink-Rise system, north Florida, USA. *Journal of Geophysical Research: Biogeosciences*, *119*, 340–357. https://doi.org/10.1002/2013JG002350

Kirchner, J. W., & Neal, C. (2013). Universal fractal scaling in stream chemistry and its implications for solute transport and water quality trend detection. *Proceedings of the National Academy of Sciences of the United States of America*, *110*(30), 12,213–12,218. https://doi.org/10.1073/pnas.1304328110

Li, G., Hartmann, J., Derry, L. A., West, A. J., You, C.-F., Long, X., et al. (2016). Temperature dependence of basalt weathering. *Earth and Planetary Science Letters*, *443*, 59–69. https://doi.org/10.1016/j.epsl.2016.03.015

Li, S., & Bush, R. T. (2015). Changing fluxes of carbon and other solutes from the Mekong River. *Scientific Reports*, *5*(1), 16,005. https://doi.org/10.1038/srep16005

Li, S. L., Calmels, D., Han, G., Gaillardet, J., & Liu, C. Q. (2008). Sulfuric acid as an agent of carbonate weathering constrained by $\delta^{13}C_{DIC}$: Examples from Southwest China. *Earth and Planetary Science Letters*, *270*(3–4), 189–199. https://doi.org/10.1016/j.epsl.2008.02.039

Li, S. L., Liu, C. Q., Li, J., Lang, Y. C., Ding, H., & Li, L. (2010). Geochemistry of dissolved inorganic carbon and carbonate weathering in a small typical karstic catchment of Southwest China: Isotopic and chemical constraints. *Chemical Geology*, *277*(3-4), 301–309, https://doi.org/10.1016/j.chemgeo.2010.08.013.

Liu, C. Q. (2007). *Biogeochemical processes and cycling of nutrients in the Earth's surface: Chemical erosion and nutrient cycling in karstic catchments, Southwest China*. Beijing: Science Press. (in Chinese)

Liu, W., & Xing, M. (2012). Isotopic indicators of carbon and nitrogen cycles in river catchments during soil erosion in the arid loess plateau of China. *Chemical Geology*, *296-297*, 66–72. https://doi.org/10.1016/j.chemgeo.2011.12.021

Lloyd, C. E. M., Freer, J. E., Johnes, P. J., Coxon, G., & Collins, A. L. (2016). Discharge and nutrient uncertainty: Implications for nutrient flux estimation in small streams. *Hydrological Processes*, *30*(1), 135–152. https://doi.org/10.1002/hyp.10574

Maher, K., & Chamberlain, C. P. (2014). Hydrologic regulation of chemical weathering and the geologic carbon cycle. *Science*, *343*(6178), 1502–1504. https://doi.org/10.1126/science.1250770

Marx, A., Dusek, J., Jankovec, J., Sanda, M., Vogel, T., van Geldern, R., et al. (2017). A review of CO_2 and associated carbon dynamics in headwater streams: A global perspective. *Reviews of Geophysics*, *55*(2), 560–585. https://doi.org/10.1002/2016RG000547

Meybeck, M. (1979). Concentrations des eaux fluviales en éléments majeurs et apports en solution aux océans. *Revue de Géologie Dynamique et de Géographie Physique*, *21*(3), 215–246.

Moon, S., Chamberlain, C. P., & Hilley, G. E. (2014). New estimates of silicate weathering rates and their uncertainties in global rivers. *Geochimica et Cosmochimica Acta*, *134*, 257–274. https://doi.org/10.1016/j.gca.2014.02.033

Mortatti, J., & Probst, J. L. (2003). Silicate rock weathering and atmospheric/soil CO_2 uptake in the Amazon basin estimated from river water geochemistry: Seasonal and spatial variations. *Chemical Geology*, *197*(1–4), 177–196. https://doi.org/10.1016/S0009-2541(02)00349-2

Musolff, A., Fleckenstein, J. H., Rao, P. S. C., & Jawitz, J. W. (2017). Emergent archetype patterns of coupled hydrologic and biogeochemical responses in catchments. *Geophysical Research Letters*, *44*, 4143–4151. https://doi.org/10.1002/2017GL072630

Musolff, A., Schmidt, C., Selle, B., & Fleckenstein, J. H. (2015). Catchment controls on solute export. *Advances in Water Resources*, *86*, 133–146. https://doi.org/10.1016/j.advwatres.2015.09.026

National Oceanic and Atmospheric Administration/Earth System Research Laboratory-Global Monitoring Division (ESRL/GMD) (2016). Globally average marine surface annual mean CO_2 data, ESRL/GMD, Boulder, CO: Retrieved from http://www.esrl.noaa.gov/gmd/index.html, (2017).

Rai, S. K., Singh, S. K., & Krishnaswami, S. (2010). Chemical weathering in the plain and peninsular sub-basins of the Ganga: Impact on major ion chemistry and elemental fluxes. *Geochimica et Cosmochimica Acta*, *74*(8), 2340–2355. https://doi.org/10.1016/j.gca.2010.01.008

Ran, L., Lu, X. X., Sun, H., Han, J., Li, R., & Zhang, J. (2013). Spatial and seasonal variability of organic carbon transport in the Yellow River, China. *Journal of Hydrology*, *498*, 76–88. https://doi.org/10.1016/j.jhydrol.2013.06.018

Raymond, P. A. (2017). Temperature versus hydrologic controls of chemical weathering fluxes from United States forests. *Chemical Geology*, *458*, 1–13. https://doi.org/10.1016/j.chemgeo.2017.02.025

Raymond, P. A., Hartmann, J., Lauerwald, R., Sobek, S., McDonald, C., Hoover, M., et al. (2013). Global carbon dioxide emissions from inland waters. *Nature*, *503*(7476), 355–359. https://doi.org/10.1038/nature12760

Raymond, P. A., & Oh, N.-H. (2007). An empirical study of climatic controls on riverine C export from three major U.S. watersheds. *Global Biogeochemical Cycles*, *21*, GB2022. https://doi.org/10.1029/2006GB002783

Raymond, P. A., Oh, N.-H., Turner, R. E., & Broussard, W. (2008). Anthropogenically enhanced fluxes of water and carbon from the Mississippi River. *Nature*, *451*(7177), 449–452. https://doi.org/10.1038/nature06505

Reichstein, M., Bahn, M., Ciais, P., Frank, D., Mahecha, M. D., Seneviratne, S. I., et al. (2013). Climate extremes and the carbon cycle. *Nature*, *500*(7462), 287–295. https://doi.org/10.1038/nature12350

Rue, G. P., Rock, N. D., Gabor, R. S., Pitlick, J., Tfaily, M., & McKnight, D. M. (2017). Concentration-discharge relationships during an extreme event: Contrasting behavior of solutes and changes to chemical quality of dissolved organic material in the Boulder Creek Watershed during the September 2013 flood. *Water Resources Research*, *53*, 5276–5297. https://doi.org/10.1002/2016WR019708

Runkel, R.L., Crawford, C.G., & Cohn, T.A. (2004). LoadEstimator (LOADEST): A FORTRAN program for estimating constituent loads in streams and rivers. U.S. Geological Survey techniques and methods Book 4, chapter A5. Reston, VA. Retrieved from http://water.usgs.gov/software/loadest.

Sun, H., Han, J., Li, D., Zhang, S., & Lu, X. (2010). Chemical weathering inferred from riverine water chemistry in the lower Xijiang basin, South China. *The Science of the Total Environment*, *408*(20), 4749–4760. https://doi.org/10.1016/j.scitotenv.2010.06.007

Sun, H., Han, J., Lu, X. X., Zhang, S. R., & Li, D. (2010). An assessment of the riverine carbon flux of the Xijiang River during the past 50 years. *Quaternary International*, *226*(1–2), 38–43. https://doi.org/10.1016/j.quaint.2010.03.002

Sun, H., Han, J., Zhang, S., & Lu, X. (2007). The impacts of '05.6' extreme flood event on riverine carbon fluxes in Xijiang River. *Chinese Science Bulletin*, *52*(6), 805–812. https://doi.org/10.1007/s11434-007-0111-6

Sun, H., Liu, Z., Yang, R., Chen, B., Yang, M., & Zeng, Q. (2017). Spatial and seasonal variations of hydrochemistry of the Peral River and implications for estimating the rock weathering-related carbon sink (in Chinese). *Earth and the Environment*, *45*(1), 57–65.

Szramek, K., McIntosh, J. C., Williams, E. L., Kanduc, T., Ogrinc, N., & Walter, L. M. (2007). Relative weathering intensity of calcite versus dolomite in carbonate-bearing temperate zone watersheds: Carbonate geochemistry and fluxes from catchments within the St. Lawrence and Danube river basins. *Geochemistry, Geophysics, Geosystems*, *8*, Q04002. https://doi.org/10.1029/2006GC001337

Telmer, K., & Veizer, J. (1999). Carbon fluxes, pCO_2 and substrate weathering in a large northern river basin, Canada carbon isotope perspectives. *Chemical Geology*, *159*(1-4), 61–86. https://doi.org/10.1016/S0009-2541(99)00034-0

Thompson, S. E., Basu, N. B., Lascurain, J., Aubeneau, A., & Rao, P. S. C. (2011). Relative dominance of hydrologic versus biogeochemical factors on solute export across impact gradients. *Water Resources Research*, *47*, W00J05. https://doi.org/10.1029/2010WR009605

Tipper, E. T., Bickle, M. J., Galy, A., West, A. J., Pomiès, C., & Chapman, H. J. (2006). The short term climatic sensitivity of carbonate and silicate weathering fluxes: Insight from seasonal variations in river chemistry. *Geochimica et Cosmochimica Acta*, *70*(11), 2737–2754. https://doi.org/10.1016/j.gca.2006.03.005

Torres, M. A., Baronas, J. J., Clark, K. E., Feakins, S. J., & West, A. J. (2016). Mixing as a driver of temporal variations in river hydrochemistry: 1. Insights from conservative tracers in the Andes-Amazon transition. *Water Resources Research*, *53*, 3102–3119. https://doi.org/10.1002/2016WR019733

Torres, M. A., West, A. J., & Clark, K. E. (2015). Geomorphic regime modulates hydrologic control of chemical weathering in the Andes-Amazon. *Geochimica et Cosmochimica Acta*, *166*, 105–128. https://doi.org/10.1016/j.gca.2015.06.007

Voss, B. M., Peucker-Ehrenbrink, B., Eglinton, T. I., Fiske, G., Wang, Z. A., Hoering, K. A., et al. (2014). Tracing river chemistry in space and time: Dissolved inorganic constituents of the Fraser River, Canada. *Geochimica et Cosmochimica Acta*, *124*, 283–308. https://doi.org/10.1016/j.gca.2013.09.006

Waldron, S., Scott, E. M., & Soulsby, C. (2007). Stable isotope analysis reveals lower-order river dissolved inorganic carbon pools are highly dynamic. *Environmental Science & Technology*, *41*(17), 6156–6162. https://doi.org/10.1021/es0706089

Wang, Z., Ma, J., Li, J., Wei, G., Chen, X., Deng, W., et al. (2015). Chemical weathering controls on variations in the molybdenum isotopic composition of river water: Evidence from large rivers in China. *Chemical Geology*, *410*, 201–212. https://doi.org/10.1016/j.chemgeo.2015.06.022

Ward, N. D., Keil, R. G., Medeiros, P. M., Brito, D. C., Cunha, A. C., Dittmar, T., et al. (2013). Degradation of terrestrially derived macromolecules in the Amazon River. *Nature Geoscience*, *6*(7), 530–533. https://doi.org/10.1038/NGEO1817

Wei, G., Ma, J., Liu, Y., Xie, L., Lu, W., Deng, W., et al. (2013). Seasonal changes in the radiogenic and stable strontium isotopic composition of Xijiang River water: Implications for chemical weathering. *Chemical Geology*, *343*, 67–75. https://doi.org/10.1016/j.chemgeo.2013.02.004

West, A. J., Galy, A., & Bickle, M. (2005). Tectonic and climatic controls on silicate weathering. *Earth and Planetary Science Letters*, *235*, 211–228. https://doi.org/10.1016/j.epsl.2005.03.020

Xu, Z., & Liu, C. Q. (2007). Chemical weathering in the upper reaches of Xijiang River draining the Yunnan-Guizhou Plateau, Southwest China. *Chemical Geology*, *239*(1–2), 83–95. https://doi.org/10.1016/j.chemgeo.2006.12.008

Xu, Z., & Liu, C. Q. (2010). Water geochemistry of the Xijiang basin rivers, South China: Chemical weathering and CO_2 consumption. *Applied Geochemistry*, *25*(10), 1603–1614. https://doi.org/10.1016/j.apgeochem.2010.08.012

Zhang, H. B., Yu, S., He, S. Y., Liu, Q., & Li, Y. L. (2012). Analysis on the chemical characteristics of the atmospheric precipitation in China (in Chinese). *Carsologica Sinica*, *31*(3), 289–295.

Zhang, L., Qin, X., Liu, P., Huang, Q., Lan, F., & Ji, H. (2014). Estimation of carbon sink fluxes in the Pearl River basin (China) based on a water–rock–gas–organism interaction model. *Environment and Earth Science*, *74*(2), 945–952. https://doi.org/10.1007/s12665-014-3788-2

Zhang, Q., Harman, C. J., & Ball, W. P. (2016). An improved method for interpretation of riverine concentration-discharge relationships indicates long-term shifts in reservoir sediment trapping. *Geophysical Research Letters*, *43*, 10,215–10,224. https://doi.org/10.1002/2016GL069945

Zhang, S. R., Lu, X., Higgitt, D. L., Chen, C. T. A., Sun, H. G., & Han, J. T. (2007). Water chemistry of the Zhujiang (Pearl River): Natural processes and anthropogenic influences. *Journal of Geophysical Research*, *112*, F01011. https://doi.org/10.1029/2006JF000493

Zhong, J., Li, S. L., Tao, F., Ding, H., & Liu, J. (2017). Impacts of hydrologic variations on chemical weathering and solute sources in the Min River basin, Himalayan-Tibetan region. *Environemental Science and Pollution Research*, *24*, 19,126–19,137. https://doi.org/10.1007/s11356-017-9584-2

Zhong, J., Li, S. L., Tao, F., Yue, F., & Liu, C. Q. (2017). Sensitivity of chemical weathering and dissolved carbon dynamics to hydrological conditions in a typical karst river. *Scientific Reports*, *7*(1), 42,944. https://doi.org/10.1038/srep42944